# Two-photon dynamics in non-Markovian waveguide QED with a giant atom

Wenju Gu,* Tao Li, Ye Tian, and Zhen Yi
*School of Physics and Optoelectronic Engineering, Yangtze University, Jingzhou 434023, China*

Gao-xiang Li†
*Department of Physics, Huazhong Normal University, Wuhan 430079, China*

(Received 26 June 2024; accepted 26 August 2024; published 9 September 2024)

We investigate one- and two-photon scattering in a one-dimensional waveguide coupled to a giant atom within the non-Markovian regime using the resolvent approach. The non-Markovian behavior gives rise to an atom-photon bound state that cannot be excited by a single incident photon. However, the bound state can be excited via the two-photon scattering process described by multichannel scattering theory, from which an analytical trapping probability of a photon in the bound state can be achieved. Additionally, we analyze the two-photon scattering process, obtaining the analytical expressions for scattered states. As non-Markovian effects strengthen, two peaks appear in the incoherent power spectrum, attributed to the system behaving as a leaky cavity formed by the giant atom's coupling points. Through the analysis of second-order correlation functions, we observe the bunching behavior for transmitted photons, antibunching behavior for reflected photons, and the distinctive retrieval behavior at the coupling points' separation.

DOI: 10.1103/PhysRevA.110.033707

## I. INTRODUCTION

In atom-waveguide systems, the manipulation of photons and the exploration of fundamental physics related to strong light-atom interactions and atom-mediated photon-photon interactions are of significant importance [1–3]. These studies demonstrate promising applications towards quantum communications and quantum networks [4–7]. In waveguide quantum electrodynamics (WQED) systems within the Markovian approximation, the coupling between emitters and the waveguide mode is frequency independent, and various phenomena, such as the generation of entanglement [8–11], superradiance, and subradiance [12–14], have been intensively investigated. Conversely, some theoretical interests have shifted towards exploring the physics of non-Markovian WQED systems [15–17], which exhibit a diverse range of novel physical phenomena, including non-Markovian superradiance and subradiance [12,18–21], as well as the generation of highly entangled states [22–24]. There have been some proposals and experimental implementations of non-Markovian systems using circuit QED [25] and cold atoms [26]. Of particular interest in non-Markovian WQED systems is the existence of single-excitation polaritonic bound states, which are normalized eigenstates of the WQED Hamiltonian. These bound states have been extensively investigated in systems where the waveguide mode possesses a band gap, with the energy of the bound state falling within this gap [27,28]. Moreover, certain non-Markovian WQED systems can support bound states at frequencies that can propagate in the waveguide, known as bound states in the continuum [29,30]. Although exciting these bound states with single-photon wave packets is unfeasible, interactions between photons mediated by emitters can be leveraged to excite them using two-photon states [16,29]. This capability presents opportunities for storing quantum information carried by two-photon wave packets into these bound states.

Additionally, conventional atom-photon interactions have primarily focused on the small-atom regime, where interactions are confined to localized regions due to the atoms being significantly smaller than the wavelength of photons. Recently, some researches have shifted towards investigating a novel paradigm termed "giant atom," characterized by nonlocal couplings [31–37]. This configuration has been achieved by coupling artificial atoms to propagating fields, such as surface acoustic waves (SAWs), with wavelengths smaller than atomic sizes [38], or by utilizing meandering waveguides at separated points [39]. In Markovian giant-atom systems, the time for radiation to traverse the atom is much shorter than the interaction duration with the atom. Conversely, in the non-Markovian regime, giant atoms interact with the radiation field at a timescale comparable to that required for radiation to propagate across the atom. This leads to nontrivial phenomena such as nonexponential decay [38,40,41], oscillating bound states [42,43], and disentanglement dynamics [44].

In this study, we explore one- and two-photon scattering in a one-dimensional (1D) waveguide interacting with a giant atom within the non-Markovian regime. Our analysis is based on the resolvent approach. The non-Markovian nature of the system gives rise to the atom-photon bound state in a one-photon Hamiltonian, which cannot be excited by a single incident photon. However, this bound state can be excited in the two-photon scattering process, necessitating

*Contact author: guwenju@yangtzeu.edu.cn
†Contact author: gaox@mail.ccnu.edu.cn

 

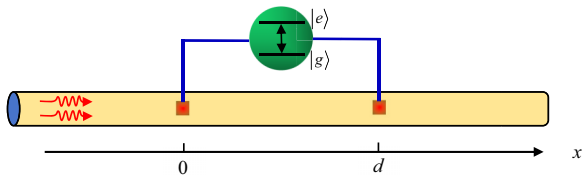


FIG. 1. Schematic illustration of a two-level giant atom side coupled to a one-dimensional (1D) waveguide. The atomic transition of the ground state $|g\rangle$ and the excited state $|e\rangle$ is coupled to waveguide modes at positions at $x = 0$ and $d$.

the application of multichannel scattering theory. By deriving multichannel scattering matrix elements which utilize the solution of a Fredholm integral equation of the second kind, we obtain an analytical expression that effectively predict the trapping rate of a photon in the atom-photon bound state. Furthermore, we extend our analysis to encompass the two-photon scattering process and obtain the analytical form of the $S$ matrix and, consequently, analytical expressions of scattered states. As the non-Markovian effects intensify, two peaks emerge in the incoherent power spectrum. This behavior can be explained by considering this system as a leaky cavity formed by two coupling points of the giant atom. Through calculations of the second-order correlation function, we find that the transmitted photons exhibit bunching behavior, reflected photons display antibunching behavior, and both exhibit distinctive retrieval behavior at the separation of coupling points.

The paper is structured as follows. In Sec. II, we introduce the physical model that describes the WQED system with a giant atom. In Sec. III, we analyze the single-photon scattering and the formation of bound states. In Sec. IV, excitation of the bound state through two-photon scattering is studied. In Sec. V, the non-Markovian two-photon scattering processes are discussed. At last, the conclusions drawn from our study are given in Sec. VI.

## II. THE PHYSICAL MODEL

We consider a two-level giant atom interacting with an open 1D waveguide at two coupling points, as shown in Fig. 1. This system can be realized in two distinct experimental configurations: a transmon qubit with multiple interdigital transducers (IDTs) coupled to SAWs through piezoelectric effects [38,45–47], or an Xmon qubit with multiple arms capacitively coupled to a coplanar waveguide [39,48]. The Hamiltonian describing the system is given by

$$\begin{aligned}\hat{H} &= \hat{H}_0 + \hat{V},\\ \hat{H}_0 &= \omega_e \hat{\sigma}_+\hat{\sigma}_- + \int_{-\infty}^{\infty} dk\, \omega_k \hat{a}_k^\dagger \hat{a}_k,\\ \hat{V} &= \sqrt{\frac{\gamma v_g}{4\pi}} \int_{-\infty}^{\infty} dk [\hat{a}_k^\dagger \hat{\sigma}_- (1 + e^{-ikd}) + \text{H.c.}],\end{aligned} \tag{1}$$

where $\omega_e$ represents the atomic transition frequency, and $\hat{\sigma}_- = |g\rangle\langle e|$ and $\hat{\sigma}_+ = |e\rangle\langle g|$ are the atomic transition operators. The frequency of the bosonic fields in the 1D waveguide follows a linear dispersion relation, i.e., $\omega_k = v_g|k|$, where $v_g$ is the group velocity and $k$ is the wave vector. The positive and negative values of $k$ correspond to right-propagating and left-propagating photons, respectively. The field operator $\hat{a}_k^\dagger$ satisfies the commutation relation $[\hat{a}_k, \hat{a}_{k'}^\dagger] = \delta(k - k')$. The giant atom couples to the waveguide at positions $x = 0$ and $d$ with an identical coupling strength of $\sqrt{\frac{\gamma v_g}{4\pi}}$, where $\gamma$ is the atomic relaxation rate to waveguide modes. The time taken for photons to travel between these two coupling points is $\tau = d/v_g$. In this study, we focus on phenomena arising from non-Markovian dynamics, which become significant when the time delay $\tau$ is non-negligible.

## III. SINGLE-PHOTON SCATTERING AND FORMATION OF THE BOUND STATE

The formation of bound states confined within the coupling points is the distinction between the Markovian and the non-Markovian dynamics with giant atoms. To obtain the bound state in the one-photon sector, we employ the resolvent of the Hamiltonian [49,50], which is defined by

$$\hat{G}(z) = \frac{1}{z - \hat{H}}. \tag{2}$$

The resolvent operator $\hat{G}(z)$ satisfies the Lippmann-Schwinger (LS) equation, which is

$$\hat{G}(z) = \hat{G}_0(z) + \hat{G}_0(z)\hat{V}\hat{G}(z) = \hat{G}_0(z) + \hat{G}(z)\hat{V}\hat{G}_0(z). \tag{3}$$

Here, $\hat{G}_0(z) = 1/(z - \hat{H}_0)$ is the resolvent of the free Hamiltonian. In the one-photon sector, the waveguide states $|k\rangle$ and the atomic excited state $|e\rangle$ form a complete basis. Consequently, there exist four matrix elements of $\hat{G}(z)$, which are

$$\begin{aligned}G_1(z) &= \langle e|\hat{G}(z)|e\rangle, \quad G_2(z;k) = \langle k|\hat{G}(z)|e\rangle,\\ G_3(z;k) &= \langle e|\hat{G}(z)|k\rangle, \quad G_4(z;p,k) = \langle p|\hat{G}(z)|k\rangle.\end{aligned} \tag{4}$$

By employing the LS equation in (3), these matrix elements fulfill the following relationships:

$$\begin{aligned}G_1(z) &= \frac{1}{z - \omega_e}\left[1 + \sqrt{\frac{\gamma v_g}{4\pi}} \int_{-\infty}^{\infty} dk(1 + e^{ikd})G_2(z;k)\right],\\ G_2(z;k) &= \frac{1}{z - \omega_k}\sqrt{\frac{\gamma v_g}{4\pi}}(1 + e^{-ikd})G_1(z),\\ G_3(z;k) &= \frac{1}{z - \omega_k}\sqrt{\frac{\gamma v_g}{4\pi}}(1 + e^{ikd})G_1(z),\\ G_4(z;p,k) &= \frac{\delta(p-k)}{z - \omega_p} + \frac{1 + e^{-ipd}}{z - \omega_p}\sqrt{\frac{\gamma v_g}{4\pi}}G_3(z;k).\end{aligned} \tag{5}$$

Substituting the expression of $G_2(z;k)$ into the equation for $G_1(z)$ yields

$$G_1(z) = \frac{1}{z - \omega_e - \Sigma_1(z)}. \tag{6}$$

Here, $\Sigma_1(z) = -i\gamma(1 + e^{iz\tau})$ represents the self-energy term and its detailed calculation is presented in Appendix A. The poles of $G_1(z)$ are directly related to the bound state of the system. When a pole is real, it corresponds to an atom-photon bound state that does not decay despite the presence of a dissipative environment. In Appendix B, the poles are given as $z_n = \omega_e - i\gamma + iW_n(-\gamma\tau e^{\gamma\tau}e^{i\omega_e\tau})/\tau$, with $W_n(x)$ the $n$th branch of the Lambert W-function [51]. It can be verified that

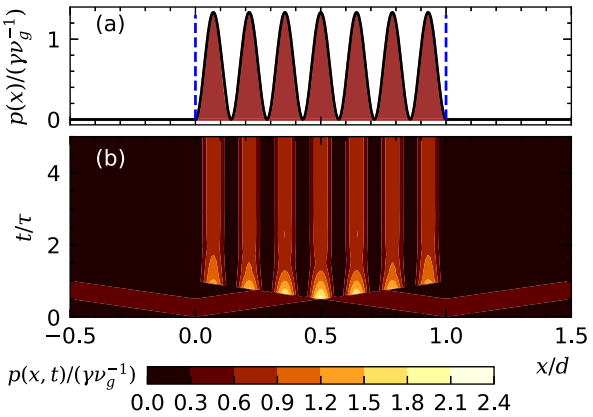


FIG. 2. Field density of the bound state. (a) Steady-state field density as a function of $x$. (b) Time evolution of field density. The parameters are $\gamma\tau = 0.5$, $\omega_e\tau = (2n+1)\pi$, and $n = 3$.

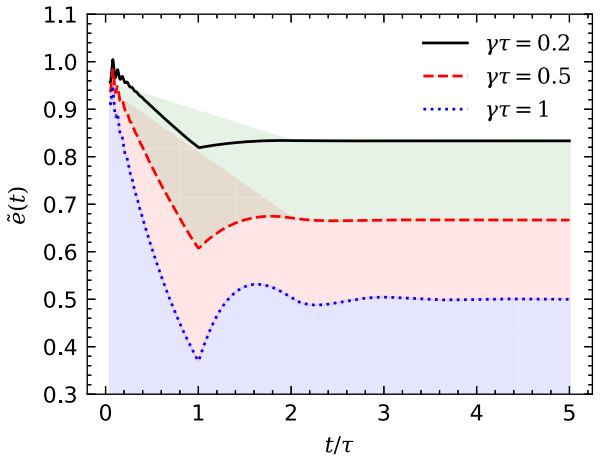


FIG. 3. Time evolution of the atomic excitation probability $\tilde{e}(t)$ with different values of $\gamma\tau$ under the condition of $\omega_e\tau = (2n+1)\pi$.

the real solution of $z$ should satisfy the conditions $z = \omega_e$ and the time delay $\tau = (2n+1)\pi/\omega_e$ [42,52,53].

To further obtain the explicit expression for the bound state, denoted as $|\psi_b\rangle$, we employ the theory of the Green's function [54]. The atomic part of the bound state is derived using the residue theorem,

$$\langle e|\psi_b\rangle\langle\psi_b|e\rangle = \mathrm{Res}[G_1(z),\omega_e] = \frac{1}{1+\gamma\tau}. \tag{7}$$

Similarly, the photonic part of the bound state is obtained through

$$\begin{aligned}\langle p|\psi_b\rangle\langle\psi_b|k\rangle &= \mathrm{Res}[G_4(z;p,k),\omega_e]\\ &= \frac{\gamma v_g}{4\pi}\frac{1}{1+\gamma\tau}\frac{(1+e^{-ipd})(1+e^{ikd})}{(\omega_e-\omega_p)(\omega_e-\omega_k)}.\end{aligned} \tag{8}$$

Combining these results yields a complete expression for the bound state,

$$|\psi_b\rangle = \sqrt{\frac{1}{1+\gamma\tau}}\left[|e\rangle + \sqrt{\frac{\gamma v_g}{4\pi}}\int_{-\infty}^{\infty} dk\,\frac{1+e^{-ikd}}{\omega_e-\omega_k}|k\rangle\right]. \tag{9}$$

To represent the bound state in real space, we utilize the transformation

$$|x\rangle = \frac{1}{\sqrt{2\pi}}\int_{-\infty}^{\infty} dk e^{-ikx}|k\rangle. \tag{10}$$

Consequently, the bound state in real space is given by

$$|\psi_b\rangle = \sqrt{\frac{1}{1+\gamma\tau}}\left[|e\rangle + \sqrt{\frac{2\gamma}{v_g}}\int_0^d dx\sin\left(\frac{\omega_e}{v_g}x\right)|x\rangle\right]. \tag{11}$$

The photon position probability density $p(x)$ is then given by

$$\begin{aligned}p(x) &= |\langle x|\psi_b\rangle|^2\\ &= \begin{cases}\frac{2\gamma}{v_g(1+\gamma\tau)}\sin^2\left(\frac{\omega_e}{v_g}x\right), & 0<x<d\\ 0, & x<0\,,\ x>d.\end{cases}\end{aligned} \tag{12}$$

It is evident that the photonic states are localized within the region between the coupling points, as illustrated in Fig. 2(a). In the context of scattering problems within the one-photon sector, the bound state does not play a significant role as its overlap with any incident wave packet is zero [22]. However, when the initial state contains the atomic contribution, the inclusion of the bound state becomes essential [12]. Here, we consider the dynamics of the system with an initially excited atom. The evolution of atomic excitation $e(t)$ and field function $\varphi(k,t)$ can be obtained through the inverse Laplace transformation,

$$\begin{aligned}e(t) &= \frac{i}{2\pi}\int_{-\infty+ia}^{\infty+ia} dz G_1(z)e^{-izt} \quad (a>0),\\ \varphi(k,t) &= \frac{i}{2\pi}\int_{-\infty+ia}^{\infty+ia} dz G_2(z;k)e^{-izt} \quad (a>0).\end{aligned} \tag{13}$$

The detailed derivation is provided in Appendix B, which gives

$$e(t) = \sum_{n\in\mathbb{Z}}\frac{e^{-iz_nt}}{1-\gamma\tau e^{iz_n\tau}}. \tag{14}$$

In the rotating frame of atomic frequency $\omega_e$, $e(t) = \tilde{e}(t)e^{-i\omega_e t}$. The time evolution of the atomic excitation probabilities $\tilde{e}(t)$ with different values of $\gamma\tau$ is presented in Fig. 3. It shows that the atom does not decay to the ground state despite the coupling to the waveguide modes, due to the existence of the bound state. In the limit of long time, $\tilde{e}(t\to\infty) = 1/(1+\gamma\tau)$. Such a phenomenon arises from the emission cancellation at the two coupling points, which fulfills the phase difference $\omega_e\tau = (2n+1)\pi$ [52].

Moreover, the evolution of the field function in real space is given by $\varphi(x,t) = \frac{1}{\sqrt{2\pi}}\int_{-\infty}^{\infty} dk e^{ikx}\varphi(k,t)$, which is

$$\begin{aligned}\varphi(x,t) = &-i\sqrt{\frac{\gamma}{2v_g}}\sum_{n\in\mathbb{Z}}\frac{e^{-iz_nt}}{1-\gamma\tau e^{iz_n\tau}}\\ &\times\{e^{iz_nx/v_g}(1+e^{-iz_n\tau})\Theta_1(t,x)\\ &+e^{-iz_nx/v_g}(1+e^{iz_n\tau})\Theta_2(t,x-d)\\ &+e^{-iz_nx/v_g}[\Theta_2(t,x)-\Theta_2(t,x-d)]\\ &+e^{iz_n(x/v_g-\tau)}[\Theta_1(t,x-d)-\Theta_1(t,x)]\},\end{aligned} \tag{15}$$

where $\Theta_1(t,x)=\theta(t-\frac{x}{v_g})-\theta(-\frac{x}{v_g})$, $\Theta_2(t,x)=\theta(t+\frac{x}{v_g})-\theta(\frac{x}{v_g})$, and $\theta(\cdot)$ is the Heaviside step function. The field density is $p(x,t)=|\varphi(x,t)|^2$. The time evolution of the field density is shown in Fig. 2(b), which is consistent with the steady-state field density in Fig. 2(a) in the the long-time limit.

Additionally, we explore the dynamics of single-photon scattering. When the frequency of the incident photon $\omega_k \neq \omega_e$, it corresponds to a scattering eigenstate that is orthogonal to the bound state. This orthogonality arises from the distinct eigenfunctions associated with different eigenvalues [55]. Furthermore, when considering the condition $\omega_k=\omega_e$, we examine the probability of atomic excitation to indicate that of the bound state by an incident photon. This analysis involves the relationship between the $S$ matrix and the $T$ operator in the one-photon sector,

$$\langle e|\hat{S}|k\rangle=-2\pi i\delta(\omega_e-\omega_k)\langle e|\hat{T}(\omega_k)|k\rangle. \tag{16}$$

The transition operator $\hat{T}$ obeys the LS equation and can be expressed in the Dyson series as

$$\hat{T}(z)=\hat{V}+\hat{V}\hat{G}_0(z)\hat{V}+\hat{V}\hat{G}_0(z)\hat{V}\hat{G}_0(z)\hat{V}+\cdots, \tag{17}$$

and we have

$$\langle e|\hat{T}(z)|k\rangle=\sqrt{\frac{\gamma v_g}{4\pi}}(1+e^{ikd})\frac{z-\omega_e}{z-\omega_e-\Sigma_1(z)}. \tag{18}$$

It can be verified that in the limit of $\omega_k\to\omega_e$, $\langle e|\hat{T}(\omega_k)|k\rangle=0$, i.e., $\langle e|\hat{S}(\omega_k)|k\rangle=0$. This indicates a complete decoupling between the regions outside and inside the coupling points [22]. In order to generate the bound state in the non-Markovian regime with significant time delays through photonic states, overlap with the photonic component of the bound state is necessary. Practically, a single photon scattered off the emitters cannot excite a bound state. This is because the incident state in the one-photon sector is always orthogonal to the bound state. However, this statement does not hold for multiphoton scattering because of the intrinsic qubit nonlinearity [29].

On the other hand, the one-photon reflection and transmission coefficients can be achieved by utilizing the relationship between the $S$ matrix and the $T$ operator,

$$\langle p|\hat{S}|k\rangle=\langle p|k\rangle-2\pi i\delta(\omega_p-\omega_k)\langle p|\hat{T}(\omega_k)|k\rangle. \tag{19}$$

The element of the $T$ operator is

$$\langle p|\hat{T}(z)|k\rangle=\frac{\gamma v_g}{4\pi}\frac{(1+e^{ikd})(1+e^{-ipd})}{z-\omega_e+i\gamma(1+e^{iz\tau})}. \tag{20}$$

We can express $\delta(\omega_p-\omega_k)$ using the properties of the delta Dirac function as

$$\delta(\omega_p-\omega_k)=[\delta(k-p)+\delta(k+p)]/v_g, \tag{21}$$

which leads to

$$\langle p|\hat{S}|k\rangle=t_p\delta(k-p)+r_p\delta(k+p). \tag{22}$$

The reflection and transmission coefficients are

$$\begin{aligned} r_p&=-i\frac{\gamma}{2}\frac{(1+e^{-ipd})^2}{\omega_p-\omega_e+i\gamma(1+e^{i\omega_p\tau})},\\ t_p&=1-i\frac{\gamma}{2}\frac{(1+e^{ipd})(1+e^{-ipd})}{\omega_p-\omega_e+i\gamma(1+e^{i\omega_p\tau})}. \end{aligned} \tag{23}$$

## IV. EXCITING THE BOUND STATE VIA TWO-PHOTON SCATTERING

In contrast to the single-photon scattering, where the bound state remains unexcited due to orthogonality with the incident state, the dynamics change with the introduction of another photon. Here, one photon can become trapped within the bound state while the other photon scatters away. In the two-photon sector, $|k_1k_2\rangle$ and $|k,e\rangle$ constitute a complete basis, and the elements of the resolvent operator are defined as follows:

$$\begin{aligned} G_5(z;p,k)&=\langle p,e|G(z)|k,e\rangle,\\ G_6(z;p_1,p_2,k)&=\langle p_1p_2|G(z)|k,e\rangle,\\ G_7(z;p,k_1,k_2)&=\langle p,e|G(z)|k_1k_2\rangle,\\ G_8(z;p_1,p_2,k_1,k_2)&=\langle p_1p_2|G(z)|k_1k_2\rangle. \end{aligned} \tag{24}$$

The orthogonality condition for the two-photon state is given by $\langle p_1p_2|k_1k_2\rangle=\delta(p_1-k_1)\delta(p_2-k_2)+\delta(p_1-k_2)\delta(p_2-k_1)$. By utilizing the LS equation in (3), we can obtain the following relationships:

$$\begin{aligned} G_5(z;p,k)&=\frac{\delta(p-k)}{z-\omega_e-\omega_p}+\frac{\sqrt{\gamma v_g/4\pi}}{z-\omega_e-\omega_p}\int_{-\infty}^{\infty}dp_i(1+e^{ip_id})G_6(z;p,p_i,k),\\ G_6(z;p_1,p_2,k)&=\frac{\sqrt{\gamma v_g/4\pi}}{z-\omega_{p_1}-\omega_{p_2}}[(1+e^{-ip_1d})G_5(z;p_2,k)+(1+e^{-ip_2d})G_5(z;p_1,k)],\\ G_7(z;p,k_1,k_2)&=\frac{\sqrt{\gamma v_g/4\pi}}{z-\omega_{k_1}-\omega_{k_2}}[(1+e^{ik_1d})G_5(z;p,k_2)+(1+e^{ik_2d})G_5(z;p,k_1)],\\ G_8(z;p_1,p_2,k_1,k_2)&=\frac{\delta(p_1-k_1)\delta(p_2-k_2)+\delta(p_2-k_1)\delta(p_1-k_2)}{z-\omega_{p_1}-\omega_{p_2}}\\ &\quad+\frac{\sqrt{\gamma v_g/4\pi}}{z-\omega_{p_1}-\omega_{p_2}}[(1+e^{-ip_1d})G_7(z;p_2,k_1,k_2)+(1+e^{-ip_2d})G_7(z;p_1,k_1,k_2)]. \end{aligned} \tag{25}$$

By defining $H(z;p) = z - \omega_e - \omega_p - \Sigma_1(z-\omega_p)$, where $\Sigma_1$ is the self-energy presented in Appendix A, the expression for $G_5(z;p,k)$ can be written as

$$H(z;p)G_5(z;p,k) = \delta(p-k) + \frac{\gamma v_g}{4\pi}(1+e^{-ipd}) \times \int_{-\infty}^{\infty} dp_i \frac{1+e^{ip_i d}}{z-\omega_p-\omega_{p_i}} G_5(z;p_i,k). \tag{26}$$

Next, we introduce the term

$$U(z;p,k) = \frac{H(z;k)[H(z;p)G_5(z;p,k) - \delta(p-k)]}{\gamma v_g/4\pi}. \tag{27}$$

This allows us to obtain the following integral equation:

$$U(z;p,k) = \frac{(1+e^{ikd})(1+e^{-ipd})}{z-\omega_p-\omega_k} + \frac{\gamma v_g}{4\pi}\int_{-\infty}^{\infty} dp_i \times \frac{(1+e^{ip_i d})(1+e^{-ipd})}{H(z;p_i)(z-\omega_p-\omega_{p_i})} U(z;p_i,k), \tag{28}$$

which is presented in terms of the solution to a linear Fredholm integral equation of the second kind. The solution of the integral equation is discussed in Appendix D

To calculate elements of the two-photon scattering scenario, we employ a multichannel scattering formalism [50]. In the two-photon sector, there exist two distinct sets of stable states that can be considered as incoming or outgoing asymptotic states within a scattering matrix framework. These sets are defined as follows: (a) Channel 0: comprising two scattered photons ($k_1$ and $k_2$) with the giant atom in its ground state. (b) Channel 1: involving one scattered photon ($p$) and a bound state formed by the photon and the giant atom. Concretely, the state of channel 0 is denoted by $|k_1k_2\rangle$ and the state of channel 1 is denoted by $|p,\psi_b\rangle$. The multichannel $S$ matrix describes transitions between these different states, and the element fulfills

$$\langle\phi_f|\hat{S}|\phi_i\rangle = \langle\phi_f|\phi_i\rangle - 2\pi i\delta(E_i-E_f)\langle\phi_f|U_{fi}(E_i)|\phi_i\rangle. \tag{29}$$

Here, $|\phi_j\rangle$ is an arbitrary asymptotic state in channel $j \in \{0,1\}$ with the energy $E_j$, and $U_{fi}(z)$ is the channel-dependent transition operator. The relationship between the resolvent $G(z)$ and $U_{fi}(z)$ is described by [56]

$$G(z) = G_f(z)\delta_{fi} + G_f(z)U_{fi}(z)G_i(z), \tag{30}$$

where $G_j(z) = 1/(z-H_j)$. Here, $G_1(z)$ is related to $H_1 = H_0 + V'$, where $V'$ is similar in form to $V$, but it acts only on the bound-state component of the wave function of channel 1 and not on the free photon part. Consequently, the operation of the resolvent $G_1(z)$ fulfills

$$G_1(z)|p,\psi_b\rangle = \frac{1}{z-\omega_p-\omega_e}|p,\psi_b\rangle. \tag{31}$$

Here, our focus is on the excitation of the bound state through the two-photon scattering, where one of the scattered photons gets trapped to form the bound state with the giant atom. Therefore, we consider the initial state consisting of two free photons as $|\phi_i\rangle = |k_1k_2\rangle$ with the energy $E_i = \omega_{k_1} + \omega_{k_2}$, and the final state as $|\phi_f\rangle = |p,\psi_b\rangle$ with the energy

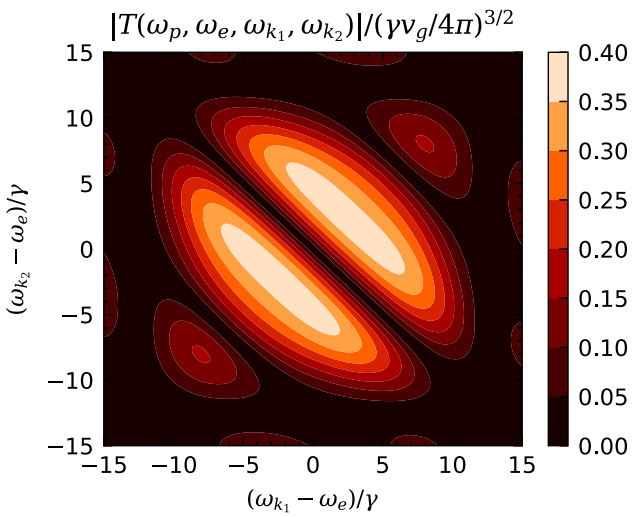


FIG. 4. The transition operator $|T(\omega_p,\omega_e,\omega_{k_1},\omega_{k_2})|$ in units of $(\gamma v_g/4\pi)^{3/2}$ as a function of $(\omega_{k_1}-\omega_e)/\gamma$ and $(\omega_{k_2}-\omega_e)/\gamma$, with $\gamma\tau = 0.5$.

$E_f = \omega_p + \omega_e$. This process is characterized by the matrix element

$$\langle p,\psi_b|S|k_1k_2\rangle = -2\pi i\delta(E_f-E_i)T\big(\omega_p,\omega_e,\omega_{k_1},\omega_{k_2}\big), \tag{32}$$

with the transition operator defined by

$$T\big(\omega_p,\omega_e,\omega_{k_1},\omega_{k_2}\big) = \langle p,\psi_b|U_{10}\big(\omega_{k_1}+\omega_{k_2}\big)|k_1k_2\rangle. \tag{33}$$

Following the detailed derivation in Appendix C, the transition operator equals

$$T\big(\omega_p,\omega_e,\omega_{k_1},\omega_{k_2}\big) = \sqrt{\frac{1}{1+\gamma\tau}}\Big(\frac{\gamma v_g}{4\pi}\Big)^{3/2}\Big[(1+e^{ik_1d}) \times \frac{U(z_{os};p,k_2)}{H(z_{os};k_2)} + k_1 \leftrightarrow k_2\Big]. \tag{34}$$

The transition operator is closely connected to $U(z;p,k)$. The solution for $U(z;p,k)$, derived from the Fredholm integral equation given in Eq. (28), is detailed in Appendix D. While obtaining an explicit solution for $U(z;p,k)$ is challenging, within the moderately non-Markovian regime where $\gamma\tau \leqslant 1$, $U(z;p,k)$ can be expressed as a Neumann series: $U(z;p,k) = \sum_{n=0}^{\infty} V_n(z;p,k)$. This series is typically solved iteratively and truncated after a few terms. As discussed in Appendix D, the approximation $U \approx V_0 + V_1$ provides a reliable prediction in the $\gamma\tau \leqslant 1$ regime. In Fig. 4, we depict the function $|T(\omega_p,\omega_e,\omega_{k_1},\omega_{k_2})|$, normalized to units of $(\gamma v_g/4\pi)^{3/2}$. The figure illustrates that it is possible to trap a photon to form the bound state, with the largest probability occurring at a slight detuning from $\omega_e$. However, when $\omega_{k_1} + \omega_{k_2} = 2\omega_e$, the bound state cannot be excited. This limitation arises from the condition $\omega_p = z_{os} - \omega_e = \omega_e$, where the transition operator is multiplied by the factor $1+e^{-ipd}$ that satisfies $1 + e^{\pm i\omega_p\tau} = 0$.

## V. THE NON-MARKOVIAN TWO-PHOTON SCATTERING PROCESS

In this section, we explore the quantum characteristics of the output field in the non-Markovian two-photon scattering process. According to Eq. (29), the scattering element is governed by the expression

$$\begin{aligned}\langle p_1 p_2|S|k_1 k_2\rangle =&\langle p_1 p_2|k_1 k_2\rangle \\ &- 2\pi i\delta\big(\omega_{p_1}+\omega_{p_2}-\omega_{k_1}-\omega_{k_2}\big)\\ &\times \langle p_1 p_2|U_{00}(z_{os})|k_1 k_2\rangle. \end{aligned} \tag{35}$$

Here, the on-shell energy fulfills $z_{os}=\omega_{p_1}+\omega_{p_2}=\omega_{k_1}+\omega_{k_2}$. Utilizing Eq. (30), we obtain

$$\begin{aligned}&\langle p_1 p_2|U_{00}(z_{os})|k_1 k_2\rangle\\ &=\sum_{m,n}(1+e^{ik_{3-m}d})(1+e^{-ip_{3-n}d})\\ &\times\left[\Big(\frac{\gamma v_g}{4\pi}\Big)^2\frac{U(z_{os};p_n,k_m)}{H(z_{os};p_n)H(z_{os};k_m)}+\frac{\gamma v_g}{4\pi}\frac{\delta(p_n-k_m)}{H(z_{os};p_n)}\right],\end{aligned} \tag{36}$$

where $m,n\in\{1,2\}$ denote photon indices, resulting in four distinct pairings of $(k_m,p_n)$ in the summation above. In the previous discussion, we have shown that $U(z_{os};p_n,k_m)$ can be expanded in a Neumann series. For the term $V_0(z_{os};p_n,k_m)=(1+e^{ik_md})(1+e^{-ip_nd})/(z_{os}-\omega_{p_n}-\omega_{k_m})$, through the use of the Sokhotski-Plemelj theorem, we have

$$\begin{aligned}\frac{1}{z_{os}-\omega_{p_n}-\omega_{k_m}}=&\mathcal{P}\frac{1}{z_{os}-\omega_{p_n}-\omega_{k_m}}\\ &-i\pi\delta\big(z_{os}-\omega_{p_n}-\omega_{k_m}\big),\end{aligned} \tag{37}$$

where $\mathcal{P}$ refers to the principal value. By extracting a delta Dirac function, the remaining terms with the principal value are denoted as $U'(z_{os};p_n,k_m)$, which is

$$\begin{aligned}U'(z_{os};p_n,k_m)=&\mathcal{P}\frac{(1+e^{ik_md})(1+e^{-ip_nd})}{z_{os}-\omega_{p_n}-\omega_{k_m}}\\ &+V_1(z_{os};p_n,k_m)+\cdots.\end{aligned} \tag{38}$$

By now, for the $\delta$ term, we have $\delta(z_{os}-\omega_{p_n}-\omega_{k_m})=\delta(\omega_{p_{3-n}}-\omega_{k_{3-m}})$. With the use of the relation $\delta(\omega_{p_{3-n}}-\omega_{k_{3-m}})=[\delta(p_{3-n}-k_{3-m})+\delta(p_{3-n}+k_{3-m})]/v_g$, we can derive the single-photon reflection and transmission amplitudes,

$$\begin{aligned}r_{p_n}&=-i\frac{\gamma}{2}\frac{(1+e^{-ip_nd})^2}{H(z_{os};p_{3-n})},\\ t_{p_n}&=1-i\frac{\gamma}{2}\frac{(1+e^{ip_nd})(1+e^{-ip_nd})}{H(z_{os};p_{3-n})},\end{aligned} \tag{39}$$

which are consistent with Eq. (23). The element of the $S$ matrix eventually takes the form

$$\begin{aligned}&\langle p_1 p_2|S|k_1 k_2\rangle\\ &=t_{p_1}t_{p_2}[\delta(p_1-k_1)\delta(p_2-k_2)+\delta(p_1-k_2)\delta(p_2-k_1)]\\ &+r_{p_1}r_{p_2}[\delta(p_1+k_1)\delta(p_2+k_2)+\delta(p_1+k_2)\delta(p_2+k_1)]\\ &+t_{p_1}r_{p_2}[\delta(p_1-k_1)\delta(p_2+k_2)+\delta(p_1-k_2)\delta(p_2+k_1)]\\ &+r_{p_1}t_{p_2}[\delta(p_1+k_1)\delta(p_2-k_2)+\delta(p_1+k_2)\delta(p_2-k_1)]\\ &+B(p_1,p_2;k_1,k_2)\delta\big(\omega_{p_1}+\omega_{p_2}-\omega_{k_1}-\omega_{k_2}\big).\end{aligned} \tag{40}$$

Here, the first four terms correspond to the coherent scattering, while the last term represents the bound-state contribution that is

$$\begin{aligned}B(p_1,p_2;k_1,k_2)=&-i\frac{\gamma^2v_g^2}{8\pi}\sum_{m,n}\frac{U'(z_{os};p_n,k_m)}{H(z_{os};p_n)H(z_{os};k_m)}\\ &\times(1+e^{ik_{3-m}d})(1+e^{-ip_{3-n}d}),\end{aligned} \tag{41}$$

which originates from the incoherent scattering. The scattering matrix element presented here closely resembles the two-photon scattering results from Refs. [57,58], but generalized to the giant-atom WQED in the non-Markovian regime.

When considering the input state of two independent photons represented by $|k_1k_2\rangle$, the output state is

$$|\psi_f\rangle=\frac{1}{2!}\iint dp_1dp_2\langle p_1p_2|S|k_1k_2\rangle|p_1p_2\rangle. \tag{42}$$

For the scenario where the input state consists of two right-moving photons $(k_1,k_2>0)$, the transmitted field $(p_1,p_2>0)$ takes the form $t_{k_1}t_{k_2}\hat{a}_R^\dagger(\omega_{k_1})\hat{a}_R^\dagger(\omega_{k_2})|0\rangle+\int d\omega\Upsilon(\omega)\hat{a}_R^\dagger(\omega)\hat{a}_R^\dagger(z_{os}-\omega)|0\rangle$. Here,

$$\Upsilon(\omega)=B\big(\omega,z_{os}-\omega;\omega_{k_1},\omega_{k_2}\big)/2v_g^2 \tag{43}$$

by replacing $k_md=\omega_{k_m}\tau$ and $p_nd=\omega_{p_n}\tau$ in the term $B(p_1,p_2;k_1,k_2)$. This suggests the presence of the photon pair state entangled in energy, similar to that which occurs in the spontaneous parametric down-conversion (SPDC) process [59]. Similarly, the reflected field $(p_1,p_2<0)$ is $r_{k_1}r_{k_2}\hat{a}_L^\dagger(\omega_{k_1})\hat{a}_L^\dagger(\omega_{k_2})|0\rangle+\int d\omega\Upsilon(\omega)\hat{a}_L^\dagger(\omega)\hat{a}_L^\dagger(z_{os}-\omega)|0\rangle$.

### A. Incoherent power spectrum

The spectral power spectrum of the scattered field is defined as

$$S_\alpha=\int dte^{-i\omega t}\langle\psi_f|\hat{a}_\alpha^\dagger(x_0)\hat{a}_\alpha(x_0+t)|\psi_f\rangle, \tag{44}$$

where $\alpha=\{R,L\}$ and $x_0$ represents the position of the detector located far away from the scattering region. The power spectrum comprises both coherent and incoherent components. The coherent scattering component gives rise to a $\delta$ function, while the incoherent scattering component indicates the correlation of the bound state [60]. Here, we consider the incoherent power spectrum that is

$$S_\alpha^{\text{incoh}}(\omega)=4|\Upsilon(\omega)|^2, \tag{45}$$

which can be utilized as a direct indicator of photon pair generation at the frequency $\omega$.

Within the moderately non-Markovian regime where $\gamma\tau\leqslant 1$, a fundamental approximation known as the quasi-Markovian approximation is commonly employed. This approximation, mathematically equivalent to considering only the principal value of $V_0(z_{os};p_n,k_m)$ [61], can be physically explained by viewing photons propagating in the waveguide as an effective reservoir. The rapid decay of time correlations between these photons characterizes the Markovian regime. The term "quasi" is used to signify that the field values as positions of different scatters can still differ from each other by a phase factor. Therefore, neglecting the higher-order

corrections is equivalent to making the quasi-Markovian approximation. Furthermore, in the regime of the Markovian limit where $\gamma\tau \ll 1$, we can replace the phase factor by a constant, i.e., $p_n d = k_m d = \theta$. This leads to the bound-state term,

$$\Upsilon(\omega) = \frac{i\gamma^2(1+\cos\theta)^2/\pi}{[z_{os}/2 - \omega_e + i\gamma(1+e^{i\theta})][\omega - \omega_e + i\gamma(1+e^{i\theta})]} \times \frac{1}{[z_{os} - \omega - \omega_e + i\gamma(1+e^{i\theta})]}, \tag{46}$$

under the condition of $\omega_{k_1} = \omega_{k_2} = z_{os}/2$. The result is consistent with that in Ref. [60].

In Fig. 5, we plot the incoherent power spectra for various values of $\gamma\tau$. In the regime where $\gamma\tau \ll 1$, the incoherent power spectrum aligns with the Markovian approximation. However, as the time delay between the coupling points, i.e., the degree of non-Markovianity, increases, two main peaks begin to emerge. This behavior can be understood by modeling this system as a leaky cavity formed by the two coupling points of the giant atom. In this framework, the observed peaks correspond to the renormalized excitation frequencies of the effective cavity, broadened by the renormalized decay rates. As a result, distinct bound-state-like peaks appear in the incoherent power spectrum of the scattered photons, resembling cavity resonances [62]. The frequencies and linewidths of these peaks can be interpreted in terms of the poles $z_n$ in Eq. (B2). For instance, when $\gamma\tau = 1$, the peaks are primarily determined by $z_0 = \omega_e + 1.26 - 0.35i$. Similarly, for $\gamma\tau = 2$, $z_0 = \omega_e + 0.8 - 0.1i$. As the parameter $\gamma\tau$ increases further, these main peaks shift closer to $\omega_e$ and become sharper, indicating a reduction in the effective cavity linewidth, approximately proportional to $1/(\gamma\tau)$. This shift suggests that the effective cavity resonances approach the resonance of the two-level system, thereby improving the reflectivity of the atomic coupling points and increasing the quality factor of the effective cavity. Additionally, higher-order peaks begin to emerge. For example, when $\gamma\tau = 5$, we find that the peaks are determined by $z_0 = \omega_e + 0.4 - 0.01i$ and $z_1 = \omega_e + 0.66 - 0.03i$, $z_{-1} = \omega_e + 1.5 - 0.1i$. Furthermore, when $\gamma\tau = 10$, the peaks are governed by $z_0 = \omega_e + 0.2 - 0.002i$, $z_1 = \omega_e + 0.36 - 0.006i$, $z_{-1} = \omega_e + 0.8 - 0.02i$, and $z_{-2} = \omega_e + 1.4 - 0.05i$.

Moreover, the quasi-Markovian results show good agreement with the exact solution when $\gamma\tau \ll 1$. However, as the time delay increases ($\gamma\tau \geqslant 1$), discrepancies between the approximate and exact solutions begin to emerge. One difference is that the quasi-Markovian theory tends to overestimate scattering into the incoming frequency states near $\omega = \omega_e$, as seen for $\gamma\tau = 5$ and 10 in Fig. 5. This overestimation arises because, unlike the exact solution which accounts for infinitely many excursions of photons to the atom, the quasi-Markovian approximation assumes that each photon undergoes only a single scattering event before leaving the system. As a result, the quasi-Markovian approach yields a more elastic scattering result compared to the exact solution [63]. Another difference is that the higher-order peaks resulting from inelastic scattering become more pronounced in the exact solution, as highlighted in the insets of Fig. 5. These differences underscore the importance of fully accounting for the non-Markovian effects in accurately describing the scattering dynamics.

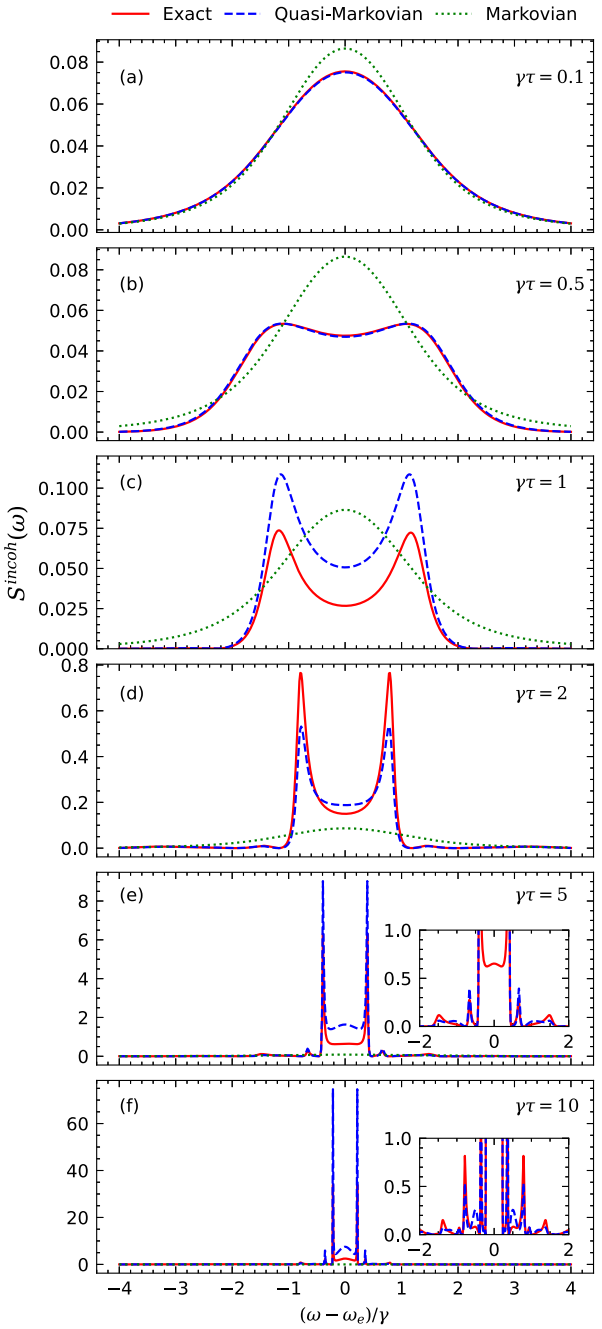


FIG. 5. Incoherent power spectra for different values of (a) $\gamma\tau = 0.1$, (b) $\gamma\tau = 0.5$, (c) $\gamma\tau = 1$, (d) $\gamma\tau = 2$, (e) $\gamma\tau = 5$, and (f) $\gamma\tau = 10$. The red solid, blue dashed, and green dot-dashed lines indicate the exact, quasi-Markovian, and Markovian solutions. The other parameters are $\omega_e\tau = (2n + 1/4)\pi$ and $\omega_{k_1} = \omega_{k_2} = \omega_e$.

### B. Second-order correlation function

By utilizing the Fourier transforms $\hat{a}_R^\dagger(\omega) = 1/\sqrt{2\pi v_g}\int dx \hat{a}_R^\dagger(x)e^{i\omega x/v_g}$ and $\hat{a}_L^\dagger(\omega) = 1/\sqrt{2\pi v_g}\int dx \hat{a}_L^\dagger(x)e^{-i\omega x/v_g}$, we can express the two-photon

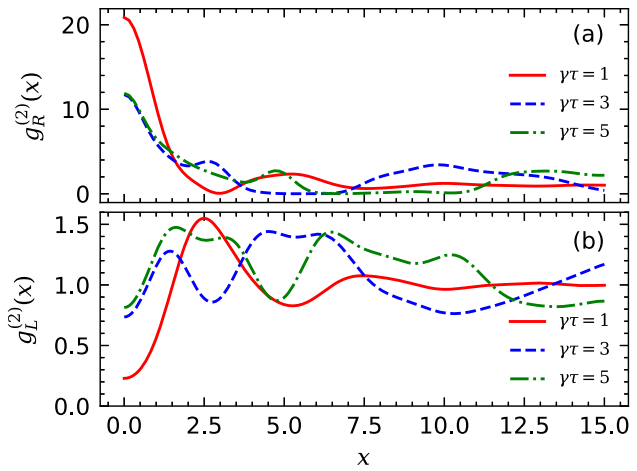


FIG. 6. Second-order correlation functions of (a) transmitted and (b) reflected photons for different values of $\gamma\tau = 1, 3$, and 5. The other parameters are $\omega_e\tau = (2n + 1/4)\pi$ and $\omega_k = \omega_e$.

state $|\psi_f\rangle$ in real space, which is

$$|\psi_f\rangle = \int dx_1 dx_2 \Bigg[ \frac{f_{RR}(x_1, x_2)}{\sqrt{2}} \hat{a}_R^\dagger(x_1)\hat{a}_R^\dagger(x_2) + \frac{f_{LL}(x_1, x_2)}{\sqrt{2}} \hat{a}_L^\dagger(x_1)\hat{a}_L^\dagger(x_2) + f_{RL}(x_1, x_2)\hat{a}_R^\dagger(x_1)\hat{a}_L^\dagger(x_2) \Bigg] |0\rangle. \tag{47}$$

Under the condition of identical frequencies for the incident photons, i.e., $\omega_{k_1} = \omega_{k_2} = \omega_k$, the two-photon transmission and reflection amplitudes are given by

$$f_{RR}(x_1, x_2) = \frac{e^{iz_{\omega_k} x_c}}{2\pi v_g}\left[t_k^2 + B_k(x)\right],$$
$$f_{LL}(x_1, x_2) = \frac{e^{-iz_{\omega_k} x_c}}{2\pi v_g}\left[r_k^2 + B_k(x)\right],$$
$$B_k(x) = \int d\omega \Upsilon(\omega) e^{i(\omega - z_{\omega_k}/2)|x|/v_g}, \tag{48}$$

where $x_c = (x_1 + x_2)/2$ and $x = x_1 - x_2$. The normalized second-order correlation functions are

$$g_R^{(2)}(x) = \left|1 + B_k(x)/t_k^2\right|^2,$$
$$g_L^{(2)}(x) = \left|1 + B_k(x)/r_k^2\right|^2. \tag{49}$$

The plots of the normalized second-order correlation functions of the transmitted and reflected photons are shown in Fig. 6. For transmitted photons, $g_R^{(2)}(0) > 1$, indicating super-Poissonian statistics where the photons tend to bunch together. Actually, this result is consistent with the expected enhancement in power extinction at zero detuning [64,65]. On the other hand, for the reflected photons, $g_L^{(2)}(0) < 1$, illustrating the antibunching behavior. Notably, the presence of long-range photon correlations is evident, with the second-order correlation components not decaying to unity even for delays significantly exceeding the separation between the coupling points, i.e., $x \gg d$. It is also worth noting that this correlation effect becomes more pronounced as $d$ increases, manifesting as slightly damped oscillations around unity in the correlation functions.

Additionally, the normalized second-order correlation functions $g_R^{(2)}(x)$ display peaks, while $g_L^{(2)}(x)$ show dips at the separation distance $d$ between the coupling points, especially under the condition $\gamma\tau \gg 1$. This phenomenon can again be explained by considering the scenario of a leaky cavity formed by the giant atom. When a photon gets trapped between the atom's coupling points, it can undergo reflections off the cavity's walls, resulting in the formation of the peaks in the second-order correlation function. This feature is particularly interesting because the second-order correlation function is a measurable quantity in experiments, rendering these peaks potentially observable effects.

## VI. CONCLUSIONS

To conclude, we have studied the dynamics of one- and two-photon scattering in a 1D waveguide interacting with a giant atom within the non-Markovian regime based on the resolvent approach. While the atom-photon bound state can be formed in the one-photon Hamiltonian, it cannot be excited by a single incident photon. However, by extending the scattering process to include two photons, excitation of this bound state becomes feasible. Using multichannel scattering theory, we derive an analytical expression for the trapping probability of a photon in the atom-photon bound state. Additionally, we investigate the incoherent power spectrum and photon-photon correlations in two-photon scattering process. When the non-Markovian effects become significant, two peaks emerge in the incoherent power spectrum. This behavior can be explained by considering this system as a leaky cavity formed by two coupling points of the giant atom. As for the second-order correlation function, the transmitted photons exhibit bunching behavior, while the reflected photons display antibunching behavior. Both types of photons exhibit distinctive retrieval behavior at the separation of coupling points.

## ACKNOWLEDGMENTS

This work was supported by the National Natural Science Foundation of China (Grants No. 1150403, No. 61505014, and No. 12174139), and China Higher Education Institution Industry-University-Research Innovation Fund (Grant No. 2022BC061).

## APPENDIX A: CALCULATION OF THE SELF-ENERGY $\Sigma_1(z)$

In the one-photon sector, the self-energy of the atom is given by

$$\Sigma_1(z) = \frac{\gamma v_g}{4\pi}\int_{-\infty}^{\infty} dk \frac{(1 + e^{ikd})(1 + e^{-ikd})}{z - \omega_k} = \frac{\gamma}{2\pi}\int_0^{\infty} d\omega_k \frac{(1 + e^{i\omega_k\tau})(1 + e^{-i\omega_k\tau})}{z - \omega_k}. \tag{A1}$$

The interaction primarily occurs around the atomic transition frequency $\omega_e$, and $\omega_k$ varies minimally outside this frequency range. Consequently, we can extend the lower limit of the $\omega_k$

integration to $-\infty$. By employing the residue theorem, the final result for the self-energy is $\Sigma_1(z) = -i\gamma(1 + e^{iz\tau})$.

## APPENDIX B: DETAILS FOR THE CALCULATION OF $e(t)$ AND $\varphi(x,t)$

In this Appendix, we present the analytical expressions for the time-dependent emitter excitation probability $e(t)$ as well as the field function $\varphi(x,t)$, which are the inverse Laplace transform of elements of the resolvent operator in Eq. (13). Concretely,

$$e(t) = \frac{i}{2\pi}\int_{-\infty+ia}^{\infty+ia} dz \frac{e^{-izt}}{z - \omega_e + i\gamma(1 + e^{iz\tau})} \qquad (a > 0). \tag{B1}$$

The integral can be obtained using the residue theorem, where the poles of the denominator are given by

$$z_n = \omega_e - i\gamma + iW_n(-\gamma\tau e^{\gamma\tau} e^{i\omega_e\tau})/\tau. \tag{B2}$$

Here, $W_n(z)$ represents the $n$th branch of the Lambert W-function [19]. Thus, the expression for $e(t)$ is

$$e(t) = \sum_{n\in\mathbb{Z}} \frac{e^{-iz_n t}}{1 - \gamma\tau e^{iz_n\tau}}. \tag{B3}$$

Furthermore, the time-dependent field function $\varphi(k,t)$ in the waveguide is given by

$$\begin{aligned}\varphi(k,t) &= \frac{i}{2\pi}\int_{-\infty+ia}^{\infty+ia} dz G_2(z;k) e^{-izt}, \\ &= \sqrt{\frac{\gamma v_g}{4\pi}}(1 + e^{-ikd})\left[\frac{e^{-i\omega_k t}}{\omega_k - \omega_e + i\gamma(1 + e^{i\omega_k\tau})}\right. \\ &\quad \left. + \sum_{n\in\mathbb{Z}} \frac{1}{z_n - \omega_k}\frac{e^{-iz_n t}}{1 - \gamma\tau e^{iz_n\tau}}\right].\end{aligned} \tag{B4}$$

The time-dependent field function in real space is expressed as

$$\varphi(x,t) = \frac{1}{\sqrt{2\pi}}\int_{-\infty}^{\infty} dk e^{ikx}\varphi(k,t). \tag{B5}$$

By employing the standard contour integral technique, the field function becomes

$$\begin{aligned}\varphi(x,t) = &-i\sqrt{\frac{\gamma}{2v_g}}\sum_{n\in\mathbb{Z}}\frac{e^{-iz_n t}}{1 - \gamma\tau e^{iz_n\tau}} \\ &\times \{e^{iz_n x/v_g}(1 + e^{-iz_n\tau})\Theta_1(t,x) \\ &+ e^{-iz_n x/v_g}(1 + e^{iz_n\tau})\Theta_2(t, x-d) \\ &+ e^{-iz_n x/v_g}[\Theta_2(t,x) - \Theta_2(t,x-d)] \\ &+ e^{iz_n(x/v_g - \tau)}[\Theta_1(t,x-d) - \Theta_1(t,x)]\},\end{aligned} \tag{B6}$$

where

$$\begin{aligned}\Theta_1(t,x) &= \theta\left(t - \frac{x}{v_g}\right) - \theta\left(-\frac{x}{v_g}\right), \\ \Theta_2(t,x) &= \theta\left(t + \frac{x}{v_g}\right) - \theta\left(\frac{x}{v_g}\right),\end{aligned} \tag{B7}$$

and $\theta(\cdot)$ is the Heaviside step function. In the limit of long time, i.e., $t \to \infty$, for the given bound state where $z_n \to \omega_e$, the field function becomes

$$\varphi(x,t) = \frac{1}{1 + \gamma\tau}\sqrt{\frac{2\gamma}{v_g}}\sin(\omega_e x/v_g). \tag{B8}$$

## APPENDIX C: CALCULATION OF THE TRANSITION OPERATOR

To obtain the explicit expression of the transition operator $T(\omega_p, \omega_e, \omega_{k_1}, \omega_{k_2})$ in Eq. (33), we utilize the relation $U_{10}(z) = G_1^{-1}(z)G(z)G_0^{-1}(z)$ and have

$$\begin{aligned}\langle p, \psi_b|U_{10}(z)|k_1k_2\rangle &= (z - \omega_p - \omega_e)(z - \omega_{k_1} - \omega_{k_2}) \\ &\quad \times \langle p, \psi_b|G(z)|k_1, k_2\rangle.\end{aligned} \tag{C1}$$

Here, according to Eq. (33), $z$ should take the on-shell energy $z_{os} \to \omega_p + \omega_e = \omega_{k_1} + \omega_{k_2}$. It should be noted that $\langle p, \psi_b|U_{10}(z_{os})|k_1k_2\rangle$ in Eq. (C1) is multiplied by two zero factors, i.e., $(z_{os} - \omega_p - \omega_e)(z_{os} - \omega_{k_1} - \omega_{k_2})$. As a result, the contribution arises from the condition of $\langle p, \psi_b|G(z)|k_1k_2\rangle$ that must have a double pole at $z_{os}$, while the other terms would approach towards zero.

Upon substituting the expression of the bound state from Eq. (9), we can obtain

$$\begin{aligned}\langle p, \psi_b|G(z)|k_1k_2\rangle = \sqrt{\frac{1}{1+\gamma\tau}}\Bigg\{&\underbrace{(1+\gamma\tau)G_7(z;p,k_1,k_2)}_{\text{term 1}} + \underbrace{\sqrt{\frac{\gamma v_g}{4\pi}}\left[\frac{1 + e^{ik_2 d}}{z - \omega_p - \omega_{k_2}}\frac{\delta(p-k_1)}{\omega_e - \omega_{k_2}} + k_1 \leftrightarrow k_2\right]}_{\text{term 2}} \\ &+ \underbrace{\frac{\gamma v_g}{4\pi}\int_{-\infty}^{\infty} dp_i \frac{1 + e^{-ipd}}{\omega_e - \omega_{p_i}}\frac{1 + e^{ip_i d}}{z - \omega_p - \omega_{p_i}} G_7(z;p_i,k_1,k_2)}_{\text{term 3}}\Bigg\}.\end{aligned} \tag{C2}$$

We will now examine these three terms individually. First, from Eq. (27), it gives

$$G_5(z;p,k) = \frac{\gamma v_g/4\pi}{H(z;k)}\frac{U(z;p,k)}{H(z;p)} + \frac{\delta(k-p)}{H(z;p)}. \tag{C3}$$

Then, substituting it into $G_7(z; p, k_1, k_2)$, and with the use of the relation

$$\lim_{z\to z_{os}} \frac{z-\omega_p-\omega_e}{H(z;p)} = \frac{1}{1+\gamma\tau}, \tag{C4}$$

for the term 1, it becomes

$$(z-\omega_p-\omega_e)\big(z-\omega_{k_1}-\omega_{k_2}\big)\times(\text{term 1}) = \Big(\frac{\gamma v_g}{4\pi}\Big)^{3/2}\Big[(1+e^{ik_1 d})\frac{U(z_{os};p,k_2)}{H(z_{os};k_2)} + k_1 \leftrightarrow k_2\Big]. \tag{C5}$$

Also, it can be verified that $(z-\omega_p-\omega_e)(z-\omega_{k_1}-\omega_{k_2})\times(\text{term 2}) = 0$ and $(z-\omega_p-\omega_e)(z-\omega_{k_1}-\omega_{k_2})\times(\text{term 3}) = 0$. As a consequence, the transition operator becomes

$$T(\omega_p,\omega_e,\omega_{k_1},\omega_{k_2}) = \sqrt{\frac{1}{1+\gamma\tau}}\Big(\frac{\gamma v_g}{4\pi}\Big)^{3/2}\Big[(1+e^{ik_1 d})\frac{U(z_{os};p,k_2)}{H(z_{os};k_2)} + k_1 \leftrightarrow k_2\Big]. \tag{C6}$$

## APPENDIX D: SOLUTION OF THE INTEGRAL EQUATION FOR $U(z_{os}; p, k)$

To achieve the solution of the integral equation for $U(z_{os}; p, k)$ as given in Eq. (28), we start by expressing $U(z_{os}; p, k)$ as

$$U(z_{os};p,k) = \tilde{U}(z_{os};p,k)(1+e^{ikd})(1+e^{-ipd}), \tag{D1}$$

where $\tilde{U}(z_{os}; p, k)$ fulfills

$$\tilde{U}(z_{os};p,k) = \frac{1}{z_{os}-\omega_p-\omega_k} + \frac{\gamma}{2\pi}\int_0^\infty d\omega_{p_i} \times \frac{(1+e^{i\omega_{p_i}\tau})(1+e^{-i\omega_{p_i}\tau})}{H(z_{os};p_i)\big(z_{os}-\omega_p-\omega_{p_i}\big)}\tilde{U}(z_{os};p_i,k). \tag{D2}$$

By closing the integration contour in the lower half plane, the term $2+e^{-i\omega_{p_i}\tau}$ in the numerator vanishes, leading to a simplified form of the equation,

$$\tilde{U}(z_{os};p,k) = \frac{1}{z_{os}-\omega_p-\omega_k} + \frac{\gamma}{2\pi}\int_0^\infty d\omega_{p_i} \times \frac{e^{i\omega_{p_i}\tau}\tilde{U}(z_{os};p_i,k)}{H(z_{os};p_i)\big(z_{os}-\omega_p-\omega_{p_i}\big)}. \tag{D3}$$

For the basic approximation, which is in the regime $\gamma\tau \leqslant 1$, we can utilize a Neumann series to solve $\tilde{U}(z_{os}; p, k) = \sum_n \tilde{V}_n(z_{os}; p, k)$ by truncating at a few orders. The zeroth-order element is

$$\tilde{V}_0(z_{os};p,k) = \frac{1}{z_{os}-\omega_p-\omega_k}, \tag{D4}$$

and the first-order element is

$$\tilde{V}_1(z_{os};p,k) = \frac{\gamma}{2\pi}\int_0^\infty d\omega_{p_i}\frac{e^{i\omega_{p_i}\tau}}{H(z_{os};p_i)\big(z_{os}-\omega_p-\omega_{p_i}\big)} \times \frac{1}{z_{os}-\omega_k-\omega_{p_i}}. \tag{D5}$$

Via employing the contour integral, it gives

$$\tilde{V}_1(z_{os};p,k) = i\gamma\Bigg\{\frac{e^{i(z_{os}-\omega_p)\tau}}{(\omega_k-\omega_p)\big[\omega_p-\omega_e+i\gamma(1+e^{i\omega_p\tau})\big]} - \frac{e^{i(z_{os}-\omega_k)\tau}}{(\omega_k-\omega_p)[\omega_k-\omega_e+i\gamma(1+e^{i\omega_k\tau})]} - \sum_{n\in\mathbb{Z}}\frac{e^{i\omega_p^{(n)}\tau}}{\big(z_{os}-\omega_p^{(n)}-\omega_p\big)\big(z_{os}-\omega_p^{(n)}-\omega_k\big)} \times \frac{1}{\big[1-\gamma\tau e^{i(z_{os}-\omega_p^{(n)})\tau}\big]}\Bigg\}, \tag{D6}$$

where $\omega_p^{(n)} = z_{os}-\omega_e+i\gamma-iW_n(-\gamma\tau e^{\gamma\tau}e^{i\omega_e\tau})/\tau$. Furthermore, the second-order element is

$$\tilde{V}_2(z_{os};p,k) = \Big(\frac{\gamma}{2\pi}\Big)^2\iint_0^\infty \frac{d\omega_{p_1}d\omega_{p_2}}{H(z_{os};p_1)(z_{os}-\omega_p-\omega_{p_1})} \times \frac{e^{i\omega_{p_1}\tau}e^{i\omega_{p_2}\tau}}{H(z_{os};p_2)(z_{os}-\omega_{p_1}-\omega_{p_2})(z_{os}-\omega_k-\omega_{p_2})}, \tag{D7}$$

which can be numerically integrated. In Fig. 7, we compare $|U(z_{os}; p, k_1)|$ with the first-order Neumann series $(\tilde{U}\approx\tilde{V}_0+\tilde{V}_1)$ and the second-order Neumann

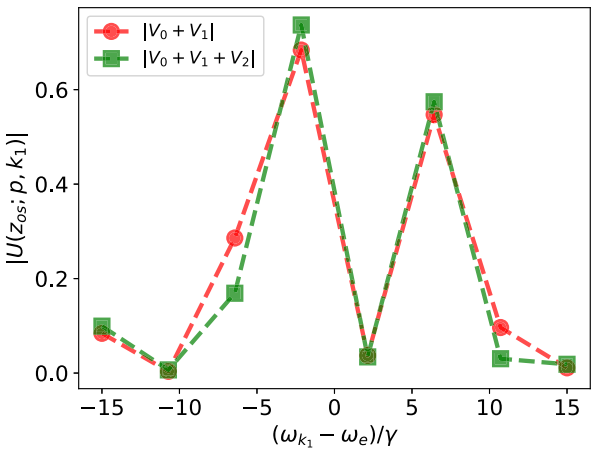


FIG. 7. Plot of $|U(z_{os}; p, k_1)|$ as a function of $(\omega_{k_1}-\omega_e)/\gamma$, with $\omega_{k_2}-\omega_e = -2\gamma$, $\omega_e = (2n+1)\pi/\tau$, $n = 3$, and $\gamma\tau = 0.5$. Red circles are for the case $\tilde{U}\approx\tilde{V}_0+\tilde{V}_1$, and green squares are for the case $\tilde{U}\approx\tilde{V}_0+\tilde{V}_1+\tilde{V}_2$.

series ($\tilde{U} \approx \tilde{V}_0 + \tilde{V}_1 + \tilde{V}_2$). The comparison reveals that the approximation $\tilde{U} \approx \tilde{V}_0 + \tilde{V}_1$ provides a reliable prediction.

In the case of a larger separation with $\gamma\tau \geqslant 1$ under the special condition where $\omega_{k_1} = \omega_{k_2} = \omega_k$, i.e., $z_{os} = 2\omega_k$, an analytical solution can be obtained as discussed in Ref. [52]. The solution is given by

$$\tilde{U}(z_{os}; p, k) = \frac{1}{\omega_k - \omega_p} + F(\omega_k - \omega_p), \tag{D8}$$

where the function $F(q)$ is defined as

$$F(q) = -\frac{i\gamma e^{i\varphi}}{\lambda + i\gamma e^{i\varphi}} \sum_{\sigma=\pm,0} C_\sigma \frac{e^{iq\tau} - e^{-i\sigma p\tau}}{q + \sigma p}. \tag{D9}$$

Here, the parameters are

$$p = \sqrt{\lambda^2 + \gamma^2 e^{i2\varphi}}, \quad \lambda = \delta + i\gamma,$$
$$\varphi = \omega_k \tau, \quad \delta = \omega_k - \omega_e,$$
$$C_\pm = \pm\frac{(\pm p - \lambda)e^{\pm ip\tau} - i\gamma e^{i\varphi}}{2(p\cos p\tau - i\lambda \sin p\tau)}, \quad C_0 = -1. \tag{D10}$$


[1] D. Roy, C. M. Wilson, and O. Firstenberg, Colloquium: Strongly interacting photons in one-dimensional continuum, Rev. Mod. Phys. **89**, 021001 (2017).

[2] A. S. Sheremet, M. I. Petrov, I. V. Iorsh, A. V. Poshakinskiy, and A. N. Poddubny, Waveguide quantum electrodynamics: Collective radiance and photon-photon correlations, Rev. Mod. Phys. **95**, 015002 (2023).

[3] X. Gu, A. F. Kockum, A. Miranowicz, Y. xi Liu, and F. Nori, Microwave photonics with superconducting quantum circuits, Phys. Rep. **718-719**, 1 (2017).

[4] H. Pichler and P. Zoller, Photonic circuits with time delays and quantum feedback, Phys. Rev. Lett. **116**, 093601 (2016).

[5] J. Kumlin, S. Hofferberth, and H. P. Büchler, Emergent universal dynamics for an atomic cloud coupled to an optical waveguide, Phys. Rev. Lett. **121**, 013601 (2018).

[6] T. Li, A. Miranowicz, X. Hu, K. Xia, and F. Nori, Quantum memory and gates using a Λ-type quantum emitter coupled to a chiral waveguide, Phys. Rev. A **97**, 062318 (2018).

[7] K. Xia, F. Nori, and M. Xiao, Cavity-free optical isolators and circulators using a chiral cross-kerr nonlinearity, Phys. Rev. Lett. **121**, 203602 (2018).

[8] G.-Q. Zhang, W. Feng, W. Xiong, D. Xu, Q.-P. Su, and C.-P. Yang, Generating Bell states and $n$-partite $w$ states of long-distance qubits in superconducting waveguide QED, Phys. Rev. Appl. **20**, 044014 (2023).

[9] C. Gonzalez-Ballestero, E. Moreno, and F. J. Garcia-Vidal, Generation, manipulation, and detection of two-qubit entanglement in waveguide QED, Phys. Rev. A **89**, 042328 (2014).

[10] I. M. Mirza and J. C. Schotland, Multiqubit entanglement in bidirectional-chiral-waveguide QED, Phys. Rev. A **94**, 012302 (2016).

[11] K. Xia, F. Jelezko, and J. Twamley, Quantum routing of single optical photons with a superconducting flux qubit, Phys. Rev. A **97**, 052315 (2018).

[12] F. Dinc, İ. Ercan, and A. M. Brańczyk, Exact Markovian and non-Markovian time dynamics in waveguide QED: Collective interactions, bound states in continuum, superradiance and subradiance, Quantum **3**, 213 (2019).

[13] S. Cardenas-Lopez, S. J. Masson, Z. Zager, and A. Asenjo-Garcia, Many-body superradiance and dynamical mirror symmetry breaking in waveguide QED, Phys. Rev. Lett. **131**, 033605 (2023).

[14] A. Albrecht, L. Henriet, A. Asenjo-Garcia, P. B. Dieterle, O. Painter, and D. E. Chang, Subradiant states of quantum bits coupled to a one-dimensional waveguide, New J. Phys. **21**, 025003 (2019).

[15] T. Shi, D. E. Chang, and J. I. Cirac, Multiphoton-scattering theory and generalized master equations, Phys. Rev. A **92**, 053834 (2015).

[16] R. Trivedi, D. Malz, S. Sun, S. Fan, and J. Vučković, Optimal two-photon excitation of bound states in non-Markovian waveguide QED, Phys. Rev. A **104**, 013705 (2021).

[17] S. Arranz Regidor, G. Crowder, H. Carmichael, and S. Hughes, Modeling quantum light-matter interactions in waveguide qed with retardation, nonlinear interactions, and a time-delayed feedback: Matrix product states versus a space-discretized waveguide model, Phys. Rev. Res. **3**, 023030 (2021).

[18] A. Carmele, N. Nemet, V. Canela, and S. Parkins, Pronounced non-Markovian features in multiply excited, multiple emitter waveguide QED: Retardation induced anomalous population trapping, Phys. Rev. Res. **2**, 013238 (2020).

[19] K. Sinha, P. Meystre, E. A. Goldschmidt, F. K. Fatemi, S. L. Rolston, and P. Solano, Non-Markovian collective emission from macroscopically separated emitters, Phys. Rev. Lett. **124**, 043603 (2020).

[20] F. Dinc and A. M. Brańczyk, Non-Markovian super-superradiance in a linear chain of up to 100 qubits, Phys. Rev. Res. **1**, 032042(R) (2019).

[21] K. Sinha, A. González-Tudela, Y. Lu, and P. Solano, Collective radiation from distant emitters, Phys. Rev. A **102**, 043718 (2020).

[22] C. Gonzalez-Ballestero, F. J. García-Vidal, and E. Moreno, Non-Markovian effects in waveguide-mediated entanglement, New J. Phys. **15**, 073015 (2013).

[23] C. A. González-Gutiérrez, J. Román-Roche, and D. Zueco, Distant emitters in ultrastrong waveguide QED: Ground-state properties and non-Markovian dynamics, Phys. Rev. A **104**, 053701 (2021).

[24] H. Zheng and H. U. Baranger, Persistent quantum beats and long-distance entanglement from waveguide-mediated interactions, Phys. Rev. Lett. **110**, 113601 (2013).

[25] V. S. Ferreira, J. Banker, A. Sipahigil, M. H. Matheny, A. J. Keller, E. Kim, M. Mirhosseini, and O. Painter, Collapse and revival of an artificial atom coupled to a structured photonic reservoir, Phys. Rev. X **11**, 041043 (2021).

[26] A. González-Tudela, C. S. Muñoz, and J. I. Cirac, Engineering and harnessing giant atoms in high-dimensional baths: A proposal for implementation with cold atoms, Phys. Rev. Lett. **122**, 203603 (2019).

[27] G. Calajó, F. Ciccarello, D. Chang, and P. Rabl, Atom-field dressed states in slow-light waveguide QED, Phys. Rev. A **93**, 033833 (2016).

[28] T. Shi, Y.-H. Wu, A. González-Tudela, and J. I. Cirac, Bound states in boson impurity models, Phys. Rev. X **6**, 021027 (2016).

[29] G. Calajó, Yao-Lung L. Fang, H. U. Baranger, and F. Ciccarello, Exciting a bound state in the continuum through multiphoton scattering plus delayed quantum feedback, Phys. Rev. Lett. **122**, 073601 (2019).

[30] L. Leonforte, A. Carollo, and F. Ciccarello, Vacancy-like dressed states in topological waveguide QED, Phys. Rev. Lett. **126**, 063601 (2021).

[31] A. F. Kockum, G. Johansson, and F. Nori, Decoherence-free interaction between giant atoms in waveguide quantum electrodynamics, Phys. Rev. Lett. **120**, 140404 (2018).

[32] A. Frisk Kockum, Quantum optics with giant atoms—The first five years, in *International Symposium on Mathematics, Quantum Theory, and Cryptography*, edited by T. Takagi, M. Wakayama, K. Tanaka, N. Kunihiro, K. Kimoto, and Y. Ikematsu (Springer, Singapore, 2021), pp. 125–146.

[33] L. Du, Y. Zhang, J.-H. Wu, A. F. Kockum, and Y. Li, Giant atoms in a synthetic frequency dimension, Phys. Rev. Lett. **128**, 223602 (2022).

[34] X. Wang, T. Liu, A. F. Kockum, H.-R. Li, and F. Nori, Tunable chiral bound states with giant atoms, Phys. Rev. Lett. **126**, 043602 (2021).

[35] Y. P. Peng and W. Z. Jia, Single-photon scattering from a chain of giant atoms coupled to a one-dimensional waveguide, Phys. Rev. A **108**, 043709 (2023).

[36] W. Gu, L. Chen, Z. Yi, S. Liu, and G.-X. Li, Tunable photon-photon correlations in waveguide QED systems with giant atoms, Phys. Rev. A **109**, 023720 (2024).

[37] H. Yu, Z. Wang, and J.-H. Wu, Entanglement preparation and nonreciprocal excitation evolution in giant atoms by controllable dissipation and coupling, Phys. Rev. A **104**, 013720 (2021).

[38] G. Andersson, B. Suri, L. Guo, T. Aref, and P. Delsing, Nonexponential decay of a giant artificial atom, Nat. Phys. **15**, 1123 (2019).

[39] B. Kannan, M. J. Ruckriegel, D. L. Campbell, A. Frisk Kockum, J. Braumüller, D. K. Kim, M. Kjaergaard, P. Krantz, A. Melville, B. M. Niedzielski, A. Vepsäläinen, R. Winik, J. L. Yoder, F. Nori, T. P. Orlando, S. Gustavsson, and W. D. Oliver, Waveguide quantum electrodynamics with superconducting artificial giant atoms, Nature (London) **583**, 775 (2020).

[40] S. Guo, Y. Wang, T. Purdy, and J. Taylor, Beyond spontaneous emission: Giant atom bounded in the continuum, Phys. Rev. A **102**, 033706 (2020).

[41] Q.-Y. Qiu, Y. Wu, and X.-Y. Lü, Collective radiance of giant atoms in non-Markovian regime, Sci. China Phys. Mech. Astron. **66**, 224212 (2023).

[42] L. Guo, A. F. Kockum, F. Marquardt, and G. Johansson, Oscillating bound states for a giant atom, Phys. Rev. Res. **2**, 043014 (2020).

[43] Z. Y. Li and H. Z. Shen, Non-Markovian dynamics with a giant atom coupled to a semi-infinite photonic waveguide, Phys. Rev. A **109**, 023712 (2024).

[44] X.-L. Yin, W.-B. Luo, and J.-Q. Liao, Non-Markovian disentanglement dynamics in double-giant-atom waveguide-QED systems, Phys. Rev. A **106**, 063703 (2022).

[45] R. Manenti, A. F. Kockum, A. Patterson, T. Behrle, J. Rahamim, G. Tancredi, F. Nori, and P. J. Leek, Circuit quantum acoustodynamics with surface acoustic waves, Nat. Commun. **8**, 975 (2017).

[46] Y. Chu, P. Kharel, W. H. Renninger, L. D. Burkhart, L. Frunzio, P. T. Rakich, and R. J. Schoelkopf, Quantum acoustics with superconducting qubits, Science **358**, 199 (2017).

[47] M. V. Gustafsson, T. Aref, A. F. Kockum, M. K. Ekström, G. Johansson, and P. Delsing, Propagating phonons coupled to an artificial atom, Science **346**, 207 (2014).

[48] A. M. Vadiraj, A. Ask, T. G. McConkey, I. Nsanzineza, C. W. Sandbo Chang, A. F. Kockum, and C. M. Wilson, Engineering the level structure of a giant artificial atom in waveguide quantum electrodynamics, Phys. Rev. A **103**, 023710 (2021).

[49] C. Cohen-Tannoudji, J. Dupont-Roc, and G. Grynberg, Nonperturbative calculation of transition amplitudes, in *Atom—Photon Interactions: Basic Process and Appilcations* (Wiley, New York, 1998), Chap. 3, pp. 165–255.

[50] S. E. Kocabaş, Effects of modal dispersion on few-photon–qubit scattering in one-dimensional waveguides, Phys. Rev. A **93**, 033829 (2016).

[51] R. M. Corless, G. H. Gonnet, D. E. G. Hare, D. J. Jeffrey, and D. E. Knuth, On the Lambert-W function, Adv. Comput. Math. **5**, 329 (1996).

[52] L. Guo, A. Grimsmo, A. F. Kockum, M. Pletyukhov, and G. Johansson, Giant acoustic atom: A single quantum system with a deterministic time delay, Phys. Rev. A **95**, 053821 (2017).

[53] L. Xu and L. Guo, Catch and release of propagating bosonic field with non-Markovian giant atom, New J. Phys. **26**, 013025 (2024).

[54] F. Lombardo, F. Ciccarello, and G. M. Palma, Photon localization versus population trapping in a coupled-cavity array, Phys. Rev. A **89**, 053826 (2014).

[55] J. J. Sakurai and J. Napolitano, *Modern Quantum Mechanics* (Cambridge University Press, Cambridge, 2020).

[56] E. Alt, P. Grassberger, and W. Sandhas, Reduction of the three-particle collision problem to multi-channel two-particle Lippmann-Schwinger equations, Nucl. Phys. B **2**, 167 (1967).

[57] J.-T. Shen and S. Fan, Strongly correlated two-photon transport in a one-dimensional waveguide coupled to a two-level system, Phys. Rev. Lett. **98**, 153003 (2007).

[58] J.-T. Shen and S. Fan, Strongly correlated multiparticle transport in one dimension through a quantum impurity, Phys. Rev. A **76**, 062709 (2007).

[59] C. Zhang, Y.-F. Huang, B.-H. Liu, C.-F. Li, and G.-C. Guo, Spontaneous parametric down-conversion sources for multiphoton experiments, Adv. Quantum Technol. **4**, 2000132 (2021).

[60] W. Gu, H. Huang, Z. Yi, L. Chen, L. Sun, and H. Tan, Correlated two-photon scattering in a one-dimensional waveguide coupled to two- or three-level giant atoms, Phys. Rev. A **108**, 053718 (2023).

[61] K. Piasotski and M. Pletyukhov, Diagrammatic approach to scattering of multiphoton states in waveguide QED, Phys. Rev. A **104**, 023709 (2021).

[62] P.-O. Guimond, M. Pletyukhov, H. Pichler, and P. Zoller, Delayed coherent quantum feedback from a scattering theory and a matrix product state perspective, Quantum Sci. Technol. **2**, 044012 (2017).

[63] M. Laakso and M. Pletyukhov, Scattering of two photons from two distant qubits: Exact solution, Phys. Rev. Lett. **113**, 183601 (2014).

[64] O. Astafiev, A. M. Zagoskin, A. A. Abdumalikov, Y. A. Pashkin, T. Yamamoto, K. Inomata, Y. Nakamura, and J. S. Tsai, Resonance fluorescence of a single artificial atom, Science **327**, 840 (2010).

[65] Y. T. Zhu, S. Xue, R. B. Wu, W. L. Li, Z. H. Peng, and M. Jiang, Spatial-nonlocality-induced non-Markovian electromagnetically induced transparency in a single giant atom, Phys. Rev. A **106**, 043710 (2022).